Nanoimprinted, magnetically assembled microcontainers for cell therapy

Gimi B [1,2*#], Kwon J[2], Trivedi K,[2] Krishnamurthy NV, Hu W,[2] and Lee JB[2]
[1] University of Texas Southwestern Medical Center – Dallas, USA [2] University of Texas at Dallas – Dallas, USA
* supervisor # barjorg@yahoo.com

INTRODUCTION

Transplanted cells can secrete molecules that directly or indirectly re-establish host function and result in tissue repair/regeneration. T.M.S. Chang first proposed that transplanted cell allo- or xeno-grafts may be enclosed in selectively permeable membranes to protect the grafts from immune rejection (Chang TMS 1964). Such bioencapsulation entails a nanoporous membrane that serves as a molecular filter, permitting the passage of useful small molecules and preventing the passage of the large molecules of the immune system. Encapsulated cell therapy has been studied in a range of disease models including cancer (Xu W 2002), diabetes (Sun YL 1996) and renal failure (Prakash S 1996), with cells been entrapped in alginate microbeads or other polymers. However, 45 years after the first report on cell encapsulation, its clinical utility has not been realized. Membrane engineering has been a major impediment to the effectiveness of immunoisolation of bioartificial and biohybrid constructs for encapsulated cell transplantation. Alginate has been the most widely used polymer for encapsulation but the polymer has a wide range of pore sizes, scavenges Ca^{2+} and Mg^{2+} thereby inhibiting ionic processes for encapsulated cells, and Ca^{2+} can be partially replaced by Na^{+} that reduces the mechanical strength of the construct (Martinsen A 1992). Recently developed multi-layered PEG hydrogels demonstrate more facile control over porosity, but the microbeads formed using this method are large and impede rapid molecular transport (Weber LM 2007).

Here we present a cell encapsulation microcontainer that is fabricated using the biocompatible epoxy SU-8, which is optically- and MRI- transparent to permit the assessment of cell function post encapsulation. The microcontainer comprises a hollow cubic base to house the cells and a nanoporous lid to complete the encapsulation. Micromagnets within the base and lid help assemble and seal the microcontainer. This microcontainer is lithographically defined, resulting in control and flexibility of size and shape and in the ability to integrate micro- and nano- biosensors. The SU-8 is mechanically and chemically stable, the fabrication approach is biofriendly. We also present a strategy for engineering membranes whereby a nanoimprint Si mold is used to imprint 15 nm wide pores in membranes on the surface of the microcontainer lids. The resulting thin nanoporous SU-8 membranes permit rapid bi-directional molecular transport, and are characterized by their mechanical strength, fault tolerance and ability to fine-tune/reproduce pore size. The nanoporous lids are designed to immunoprotect the encapsulated cells while allowing the bi-directional diffusion of gases, nutrients, cellular waste products, and therapeutic molecules secreted by the encapsulated cells.

MATERIAL AND METHODS

Microcontainer fabrication: The hollowed cubic base and the lid were fabricated separately and the lid closed the cubic base to form a microcontainer after the base was filled with its cellular payload (Figure 1). The hollowed cubic base and the lid each had two discrete components (Figure 2).

Base fabrication: The bottom structure of the base comprised 50 µm thick SU-8 photoresist that was patterned to form the bottom face of the cubic microcontainer. This SU-8 layer was not

photodeveloped to ensure uniform thickness of the next layer. Next, 200 µm thick SU-8 was spun, patterned and baked to form the four side walls of the base. The top structure of the base embedded a permanent magnet in an SU-8 mold to aid in the magnetic assembly of the microcontainer. First, 25 µm thick SU-8 was patterned to form the bottom face of the mold. Then, a Cr layer was evaporated on it to promote adhesion, on which an Au layer was evaporated to serve as a seed layer for electroplating. Next, 40 µm thick SU-8 was spun, baked and patterned to form the side walls of the mold for electroplating. CoNiMnP was electroplated to build the permanent magnets. Finally, 30 µm thick SU-8 was patterned to cover the permanent magnets. The bottom and top structures of the base were aligned and bonded together at 10 bar and 20 ºC for 20 min using a nanoimprinter.

Lid fabrication: The top structure of the lid was fabricated as follows. Rectangular nanopores were formed on a thin SU-8 layer by nanoimprinting. S1813 photoresist was spun, baked and patterned to form the SU-8 membranes. SU-8 uncovered by S1813 was etched by oxygen plasma. Then, 100 µm thick SU-8 was patterned to form 30 µm diameter hollow wells that expose the nanoporous membrane while providing structural integrity to the lid. To form the bottom structure of the lid, 25 µm thick SU-8 was patterned to form the bottom face. A Cr layer was evaporated on it to promote adhesion, on which an Au layer was evaporated to serve as a seed layer for electroplating. Next, 40 µm thick SU-8 was spun, baked and patterned to form the mold for electroplating. CoNiMnP was electroplated to build permanent magnets. Finally, 50 µm thick SU-8 was patterned to cover the permanent magnets. The bottom and top structures of the lid were aligned and bonded together at 10 bar and 20 ºC for 20 min using a nanoimprinter.

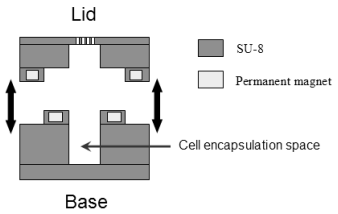

Figure 1 : The SU-8 base and the nanoporous lid of the microcontainers have permanent magnets embedded in them to aid in assembly and to close the device once it is filled with cells.

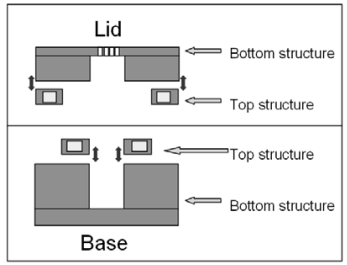

Figure 2: The based and lid each contained two discrete components that were bonded together using a nanoimprinter.

Detailed fabrication of the nanoporous membrane: Nanopores were fabricated using nanoimprint lithography (NIL). The process started with a master mold (Nanonex, Monmouth Junction, NJ) comprising 100 nm wide line gratings. Cyclical oxidation and wet etching of this master mold resulting in the desired mold for NIL with ~15 nm wide line gratings and a 200 nm pitch (Figure 3).

SU-8, spin-coated on an oxidized Si wafer, was imprinted with the master mold containing a large area of 100 nm line and space gratings. The imprinted SU-8 gratings were selectively coated with metal (Cr) by oblique angle metal evaporation so as to only coat the top of the line gratings. Next, exposed residual SU-8 was etched in inductively coupled oxygen plasma (ICP), which was

followed by ICP etching in a mixture of C_4F_8, CHF_3 and Ar to transfer patterns to the oxide layer. Then, SU-8 and Cr were removed and the profile was transferred into Si by ICP etch in chlorine. After removal of the remaining oxide mask, the resulting Si gratings were repeatedly oxidized and etched in buffered oxide etch (BOE) to gradually reduce the grating dimension. The resulting mold was used to imprint 350 nm thick SU-8 to make nanopores, around which the lid was constructed. Metal was again selectively coated on the imprinted SU-8 gratings at an angle of 35˚, followed by ICP etching in oxygen to etch exposed residual SU-8, resulting in formation of deep nano-trenches without residue. As a final step, the metal was removed and the lid structure was constructed on top of the nanopores. During plasma etching, there is a slight widening of the nanopores beyond the dimension of the top opening in the imprinted Su-8. However, due to the highly directional nature of ICP etching, the transferred dimension at the bottom of the trench is narrower than the starting dimension (Figure 4). Also, as a result of the protection provided by the metal on top of the imprinted SU-8, the top dimension of the nanopore remains unchanged. The dimension of the nanopores can be scaled down further by evaporating metal at a more oblique angle or by simply evaporating a thicker layer of metal which, in turn, reduces the gap between metal on adjacent gratings.

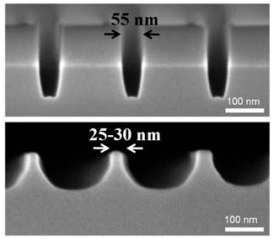

Figure 3: The nanoimprint mold (top panel) was cyclically oxidized and etched to reduce the feature size (bottom panel) until the desired 15 nm thickness was achieved.

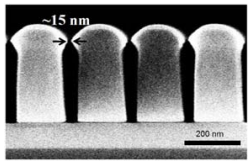

Figure 4: The imprinted SU-8 membrane had a restriction of 15 nm to serve as a molecular filter. Fault-tolerance was devised into the system by creating another restriction at the bottom of the membrane. The two restrictions in the membrane should exclude immune molecules from entering the microcontainer.

A mouse pancreatic islet was encapsulated in each of 3 microcontainers to ascertain their post encapsulation survival after 48 h. The microcontainers were maintained in cell culture medium supplemented with 15 nM FM4-64 (www.invitrogen.com) for 30 min, washed with PBS and imaged using confocal microscopy.

RESULTS AND DISCUSSION

Our MEMS-based strategy resulted in the successful fabrication of magnetically assembled, biocompatible, cell encapsulating microcontainers. We successfully bonded two discrete SU-8 components using a nanoimprinter (Figure 5). The nanoimprinting method described here resulted in a dense array of rectangular nanopores in the surface of our microcontainers with a 15 nm pore width. The nanopores can be fine tuned to effectively exclude large molecules of the immune system while permitting the transport of nutrients to the graft and cellular products from the graft to the host. Our strategy can be adapted to release other biotherapeutic molecules and drugs *in vivo*.

Encapsulated pancreatic islets survived for 48 h post encapsulation and could be visualized with the optically transparent microcontainers. The nanoporous lid permitted the transport of the small molecule FM4-64 and should therefore be effective in allowing the transport of nutrients, oxygen and hormones (Figure 6). We are currently performing long term studies of islet survival, function and immunoisolation post encapsulation.

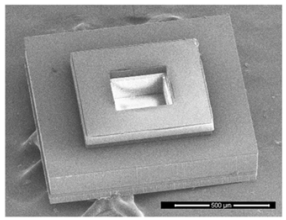

Figure 5: The two discrete components of the base were bonded together using a nanoimprinter. The resulting structure, seen above, was well-aligned so as to accommodate cells in its hollow space, and eventually the nanoporous lid. The lid was similarly bonded.

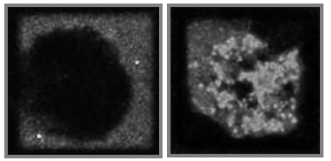

Figure 6: Islet encapsulated in the microcontainer can be easily visualized with optical methods. Confocal imaging in the green channel (left) shows no signal from the islet whereas confocal imaging in the red channel shows uptake of FM4-64 by the islet, confirming small molecule transport through the nanoporous membrane.

CONCLUSIONS

We have successfully fabricated a novel nanoporous MEMS-based microcontainer that is capable of encapsulating cells for cell based therapy. The approach may be modified to encapsulate drugs or imaging agents.

REFERENCES

• Chang TMS (1964) *Semipermeable microcapsules.* Science 146 524–525
• Martinsen A et al. (1992) *Alginate as immobilization material: III. Diffusional properties.* Biotechnol Bioeng. 39(2) 186-194
• Prakash S et al. (1996) *Microencapsulated genetically engineered live E. coli DH5 cells administered orally to maintain normal plasma urea level in uremic rats*. Nature Med. 2 883–887
• Sun YL et al. (1996) *Normalization of diabetes in spontaneously diabetic cynomologous monkeys by xenografts of microencapsulated porcine islets without immunosuppression*. J. Clin. Invest. 98 1417–1422
• Xu W et al. (2002) *Microencapsulated iNOS-expressing cells cause tumor suppression in mice*. FASEB J. 16 213–215
• Weber LM et al. (2007) *Multifunctional pancreatic islet encapsulation barriers achieved via multilayer PEG hydrogels*. Cell Transplant. 16(10) 1049-57

Acknowledgements: We acknowledge funding from NIH EB007456 and an Innovative Grant from JDRF (BG). We thank Dr. Ellen Ackerstaff for useful discussions. We thank Dr. Philip Scherer and Dr. Joyce Repa for providing islets.